Distributed Surrounding Control of Multiple Unmanned Surface Vessels With Varying Interconnection Topologies

Bin-Bin Hu, Hai-Tao Zhang, *Senior Member, IEEE*, Bin Liu, Haofei Meng, and Guanrong Chen, *Life Fellow, IEEE*

***Abstract*— In this brief, a distributed surrounding control problem is investigated for multiple unmanned surface vessels (USVs) with varying interconnection topologies. A distributed estimation-and-control hierarchical framework is developed, where an individual estimator is designed for a USV to predict the state of the target in an interconnection network with jointly dwellingly connected topologies. Thereby, the vessels could be governed to encircle the target in a convex hull, which evenly rotate around the target at the center. Moreover, asymptotical stability conditions are derived to guarantee the feasibility of the proposed surrounding controller. Finally, experiments are conducted for a real multi-USV system consisting of three 1.6 meters-long vessels and a differential GPS station, to verify the effectiveness of the proposed controller.**

***Index Terms*— Distributed control, multiagent systems, unmanned surface vessels.**

I. Introduction

RECENT decades have experienced the tremendous development of coordinative control technology for multiple autonomous unmanned surface vessels (USVs), and the increasing demands from the tasks of aquatic resource exploration, customs antismuggling, aquatic rescues, naval attacks, water area logistics, and so on. Compared to a single USV, the virtue of multi-USV systems lies in their high efficiency, good flexibility, and superb adaptivity to complex environments, large coverage areas, low maintenance cost, etc. Moreover, multi-USV systems could accomplish complex missions like ocean resource exploration, water environmental monitoring, offshore patrolling, maritime rescue, marine material delivery, and so on. Accordingly, as emerging intelligent unmanned platforms, multi-USV systems play a more and more important role in the marine and maritime tasks.

Notably, due to many theoretical and practical challenging issues in inter-USV cooperation, most existing works focused on a single vessel, regarding path planning and obstacle avoidance [1]–[3], trajectory tracking [4]–[6], anchoring, and stabilization [7]. However, due to its capability and coverage limitation, a single USV is arduous to perform complex tasks such as collective patrolling, rescuing, capturing, exploration, monitoring, and reconnaissance. Thus, it is important and necessary to develop distributed cooperative control methods for multi-USV systems.

To this end, several promising schemes have emerged in recent years, for example, formation regulation approaches with leaders [8]–[10]. However, to attain a mutual objective, this kind of costly leader–follower approaches depend on the information of the leader(s), which limit their flexibility to adapt to environmental uncertainties and weakens their robustness against external disturbances. Some other efforts were devoted to collective formation control, where USVs are driven to form desirable geometric patterns moving along prescribed paths [11]–[13]. Because of the sophisticated design of the interactive protocols for specific patterns, only a few studies considered containment control, where USVs are driven to a convex hull containing multiple targets (or leaders) [14], [15]. This task is, however, indispensable in collective marine chasing, capturing, and hunting.

To fulfill the mission of collective chasing, capturing and hunting control for multi-USV systems, it needs surrounding control strategies for multi-agent systems (MASs). In this pursuit, some investigations consider the scenarios where the states of the targets are known to all the agents. Yamaguchi [16] proposed a feedback control law, which governs multiple robots to surround a target robot. Ni & Yang [17] developed a neural network-based control approach for collective pursuing and capturing. Sepulcher *et al.* [18] designed distributed control protocols to regulate unicycles into a circular formation with all-to-all communication. Marshall *et al.* [19] generalized the circular surrounding formation control to fulfill specific practical tasks. Moreover, Sinha and Ghose [20] developed a circulation formation control law for heterogeneous MASs. Kim and Sugie [21] developed a cyclic controller to achieve a desirable pattern for a moving target in the 3-D space. Ceccarelli and Macro *et al.* [22] designed a cyclic pursuit strategy with limited visibility of onboard sensors. Li *et al.* [23] developed a cooperative circumnavigate control protocol, which guides a microsatellite group to a given planar elliptical orbit with a proper radius.

Manuscript received April 25, 2020; revised September 6, 2020 and November 17, 2020; accepted February 3, 2021. Manuscript received in final form February 4, 2021. This work was supported in part by the National Natural Science Foundation of China under Grant U1713203, Grant 51721092, Grant 61803166, and Grant 62003145; in part by National Natural Science Foundation of Hubei Province under Grant 2019CFA005; in part by the Guangdong Province Introduction of Innovative Research and Development Team under Grant 2014ZT05G304; in part by the Program for Core Technology Tackling Key Problems of Dongguan City under Grant 2019622101007; and in part by the Fundamental Research Funds for Central Universities, HUST, under Grant 2020JYCXJJ070. Recommended by Associate Editor W. He. *(Corresponding author: Hai-Tao Zhang.)*

Bin-Bin Hu, Hai-Tao Zhang, and Bin Liu are with the School of Artificial Intelligence and Automation, Key Laboratory of Image Processing and Intelligent Control, Huazhong University of Science and Technology, Wuhan 430074, China, and also with the State Key Laboratory of Digital Manufacturing Equipment and Technology, Huazhong University of Science and Technology, Wuhan 430074, China (e-mail: hbb@hust.edu.cn; zht@mail.hust.edu.cn; binliu92@hust.edu.cn).

Haofei Meng is with the School of Automation, Southeast University, Nanjing 210096, China (e-mail: hfmeng@seu.edu.cn).

Guanrong Chen is with the Department of Electrical Engineering, City University of Hong Kong, Hong Kong (e-mail: eegchen@cityu.edu.hk).

Color versions of one or more figures in this article are available at https://doi.org/10.1109/TCST.2021.3057640.

Digital Object Identifier 10.1109/TCST.2021.3057640

However, due to the high maintenance cost in real applications, more efforts are devoted to MAS control, where only some vessels know the target(s). In this endeavor, a hybrid control protocol for a complete cyclic formation was designed in [24], and a distributed cooperative control law was proposed in [25], where the target is known to only one agent. In [26], a cycle formation control was developed based on bearing-only measurements. Then, a global-orientation free protocol was designed in [27] for MASs to circumnavigate an unknown target in the 3D space. A distributed cooperative control protocol to hunt a motional object is developed in [28], for MASs with dynamically switching topologies, which were lately improved to a more practical distributed dynamic controller [29] based only on intermittent neighborhood measurements.

To date, most existing MAS surrounding control studies consider the scenario where the target information is available to all the agents [16]–[23]. However, the high maintenance cost inevitably hinders their further applications, especially to complex marine and maritime tasks. A few MAS surrounding control works have addressed the problem where only a small number of the agents have access to the target [24]–[29]. Nevertheless, most of these works can only deal with static targets by multiple agents with first-order or second-order dynamics, and the surrounding control for more realistic motional targets by USVs with under-actuated dynamics still remains unsolved. Additionally, the challenge is intensified for USV groups with intermittent communications, which are often encountered in real USV applications. Meanwhile, due to the arduousness of real implementation, experimental surrounding control study of multi-USV groups is still on the way, which is however indispensable to pave the way from theoretical design to real applications. Therefore, it is an important yet challenging task to develop a niche distributed multi-USV surrounding control protocol to encircle a moving target.

In this brief, a distributed surrounding control framework is developed with a real surrounding and hunting unmanned platform composing of three 1.6 meters-long HUSTER-12s USVs, a differential GPS station, and a dock located on the Songshan Lake, Dongguan City, Guangdong Province, China. Then, a two-stage control framework is designed for multi-USV systems, where only a small number of vessels know the moving target, for which an observer is designed to estimate the state of the target. During the control procedure of the two-stage control, the target is first surrounded by a convex hull with the vessels as vertexes in Stage 1. Afterward, all the vessels capture and evenly rotate around the target at their geographical center in Stage 2. Experiments verify the effectiveness of the designed framework.

In summary, the contribution of this brief is twofold.

1) Developing a two-stage surrounding controller for multi-USV systems with under-actuated dynamics based only on local information with intermittent inter-USV communications.
2) Verifying the effectiveness of the proposed control framework by a real experiment with a platform consisting of three 1.6 meters-long USVs and a differential GPS station located on a lake dock.

The remainder of this brief is organized as follows. In Section II, the surrounding control problem for USVs is formulated, and then a two-stage surrounding control framework is proposed. Sections III and IV design an estimator for the moving target, and accordingly propose a two-stage distributed surrounding control protocol. Then, asymptotical stability conditions are derived to guarantee the functionality of the proposed controller. Experiments are conducted in Section V to verify the effectiveness of the control framework. Finally, conclusion is drawn in Section VI.

Throughout the brief, $\mathbb{R}^n$ denotes the n-dimensional Euclidean space, $\|*\|$ is the Euclidean norm, and $(*)_{ij}$ represents the (i, j)-th entry of a matrix $*$. $\mathbf{1}_n := [1, 1, \ldots, 1]^\mathsf{T} \in \mathbb{R}^n$; $I_n := \mathrm{diag}\{1, 1, \ldots, 1\} \in \mathbb{R}^{n\times n}$ denotes the identity matrix; $\otimes$ denotes the Kronecker product; $A \succ 0$ or $A \prec 0$ means that a square matrix A is positive or negative definite, respectively.

II. Model Description and Problem Formulation

Consider a multi-USV system consisting of n vessels with the position set $q := [q_1^\mathsf{T}, q_2^\mathsf{T}, \ldots, q_n^\mathsf{T}]^\mathsf{T} \in \mathbb{R}^{2n}$, where $q_i = [x_i, y_i]^\mathsf{T} \in \mathbb{R}^2$ represents the 2-dimensional coordination of vessel i. Define the communication network of the USVs as $\mathbb{G}(\nu, \varepsilon)$, where the vessel set $\nu = 1, 2, \ldots, n$, and ε is the communication edges among vessels. Let $\mathcal{N}_i$ be the neighborhood of vessel i in $\mathbb{G}(\nu, \varepsilon)$. The symmetric adjacency matrix $A = [a_{ij}] \in \mathbb{R}^{n\times n}$ denotes an undirected graph with $a_{ij} = a_{ji}$. Here, $a_{ij} = 1$ and 0 if there is an edge or no edge between v_i and v_j, respectively. No self-loop is allowed, and hence $a_{ii} = 0$. The connection matrix for vessels and the target is $B(t) = \mathrm{diag}\{b_i\} \in \mathbb{R}^{n\times n}$, where $b_i = 1$ if target q_0 is detected by vessel i, and 0 otherwise.

Now, a dynamic model of the multi-USV system is introduced, and then the concept of surrounding control is described.

The kinetic model of USV i is

$$\dot{q}_i = J(\psi_i)\mathbf{v}_i \tag{1}$$

with

$$J(\psi_i) = \left[s_{\psi_i}, t_{\psi_i}\right], \quad s_{\psi_i} = \begin{bmatrix}\cos(\psi_i)\\ \sin(\psi_i)\end{bmatrix}, \ t_{\psi_i} = \begin{bmatrix}-\sin(\psi_i)\\ \cos(\psi_i)\end{bmatrix}. \tag{2}$$

Here, as shown in Fig. 1, ψ_i is the phase angle of vessel i in the earth reference, $\mathbf{v}_i := [u_i, v_i]^\mathsf{T} \in \mathbb{R}^2$ is the velocity vector in the body-fixed reference, u_i the surge velocity, and v_i the sway velocity. The neighbor topology of the multi-USV system is defined according to the relative positions in clockwise direction around the target, as exhibited in Fig. 1. Thus, the pre-neighbor of vessel i is defined as i^+ whereas the next-neighbor as i^-.

The dynamics model of each vessel is (see, [4])

$$\begin{cases}\dot{\psi}_i = r_i\\ \dot{u}_i = \dfrac{m_{22}}{m_{11}}v_i r_i - \dfrac{d_{11}}{m_{11}}u_i + \dfrac{\tau_{iu}}{m_{11}}\\ \dot{r}_i = \dfrac{m_{11}-m_{22}}{m_{33}}u_i v_i - \dfrac{d_{33}}{m_{33}}r_i + \dfrac{\tau_{ir}}{m_{33}}\\ \dot{v}_i = -\dfrac{m_{11}}{m_{22}}u_i r_i - \dfrac{d_{22}}{m_{22}}v_i\end{cases} \tag{3}$$

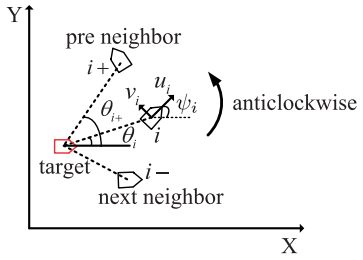

Fig. 1. Illustration of USV velocity.

where $i \in \nu$, m_{ii}, d_{ii} denote the mass and damping parameters, respectively, $\boldsymbol{\tau}_i = [\tau_{iu}, \tau_{ir}]^\mathsf{T}$ the actuator input, and r_i the yaw velocity.

Let ψ_i^r, u_i^r, v_i^r be the desired signals of ψ_i, u_i, v_i, respectively, and define

$$\widehat{\psi_i} := \psi_i - \psi_i^r, \quad \widehat{u_i} := u_i - u_i^r, \ \widehat{v_i} := v_i - v_i^r. \tag{4}$$

Substituting (4) into (1) yields

$$\dot{q}_i = \mathbf{u}_i^r + e_i \tag{5}$$

with

$$\begin{aligned} \mathbf{u}_i^r &:= J\left(\psi_i^r\right)\begin{bmatrix} u_i^r \\ v_i^r \end{bmatrix} \\ e_i &:= \left[J\left(\psi_i^r + \widehat{\psi_i}\right) - J\left(\psi_i^r\right)\right]\begin{bmatrix} u_i^r \\ v_i^r \end{bmatrix} + J(\psi_i)\begin{bmatrix} \widehat{u_i} \\ \widehat{v_i} \end{bmatrix}. \end{aligned} \tag{6}$$

Let $\mathrm{co}(\nu)$ be the convex hull of $q_1, q_2, \ldots, q_n$, that is,

$$\mathrm{co}(\nu) := \left\{ \sum_{i=1}^{n} \lambda_i q_i \,\middle|\, \lambda_i \geq 0, \sum_{i=1}^{n} \lambda_i = 1 \right\}. \tag{7}$$

Define $D_{q_0}(p) := \min_{p \in \mathrm{co}(\nu)} \|q_0(t) - p\|$ to be the distance from the target to the convex hull $\mathrm{co}(\nu)$, where $q_0(t) := [x_0(t), y_0(t)]^\mathsf{T}$ is the position of the target (see, [30]).

Next, the definitions of surrounding control and equally surrounding control are given, respectively, as below.

Definition 1 [30]: Surrounding status of the multi-USV system $\mathbb{G}(\nu, \varepsilon)$ with individual kinitic (5) is achieved once all the USVs are located in a convex hull containing the target vessel, that is,

$$\lim_{t\to\infty} D_{q_0}(t) := \min_{p \in \mathrm{co}(\nu)} \|q_0(t) - p(t)\| = 0 \tag{8}$$

with $\mathrm{co}(\nu)$ given in (7). ■

Definition 2 [30]: Equally surrounding status of the multi-USV system $\mathbb{G}(\nu, \varepsilon)$ with individual kinitic (5) is attained once the surrounding status is achieved and all the USVs evenly rotate around the target vessel, that is,

$$\begin{aligned} \lim_{t\to\infty} \rho_i &:= \|q_i - q_0\| = r \\ \lim_{t\to\infty} \theta_{i+} - \theta_i + \xi_i &= \lim_{t\to\infty} \theta_{j+} - \theta_j + \xi_j \end{aligned} \tag{9}$$

with

$$\xi_i := \begin{cases} 0, & \theta_{i+} - \theta_i \geq 0 \\ 2\pi, & \theta_{i+} - \theta_i < 0 \end{cases} \tag{10}$$

and $i, j \in \nu, i \neq j$. Here, r is the encircling radius and $\theta_i \in [0, 2\pi)$ the relative angle from vessel i to target q_0, as shown in Fig. 1. ■

To date, most existing multi-USV control efforts rely on the assumption of a connected communication topology. However, in real applications, due to external disturbances caused by waves, tides, and winds, the inter-vessel communication cannot be always guaranteed connected. Hence, USVs must be run with intermittent inter-vessel communication. To address this issue, a definition of jointly dwellingly connected is introduced.

Definition 3 [31]: Jointly dwellingly connected is satisfied if $T_c \geq \mu T$ with a specified rate $0 < \mu < 1$ and $T > 0$, where $T_c := \min\{T_j^c\}$ is the time interval sequences $[T_j, T_{j+1})$, $j = 0, 1, \ldots$, with $T_0 = t_0$, $T_{j+1} = T_j + T$. Here, T_j^c denotes the total length of the connected graphs in time interval $[T_j, T_{j+1})$. Each time interval consists of a number of sub-time intervals $[t_j, t_{j+1})$, during which the interconnection graph is time-invariant. Assume that $t_{j+1} - t_j \geq \tau$, where τ is called the dwell time. ■

Now, it is ready to propose three technical problems for study.

Problem 1 *(Surrounding Control):* Design a control signal

$$\mathbf{u}_i^r = f\left(q_i, q_j\right), \quad i \in \nu, \ j \in \mathcal{N}_i \tag{11}$$

for vessel i in a multi-USV system $\mathbb{G}(\nu, \varepsilon)$ governed by (5) to achieve the surrounding motion (see Definition 1) toward a moving target $q_0(t) \in \mathbb{R}^2$ with a constant velocity $\dot{q}_0(t) = v_0$, subject to $\lim_{t\to\infty} e_i(t) = 0$.

Problem 2 *(Equally Surrounding Control):* Design a control signal

$$\mathbf{u}_i^r = f\left(q_i, q_j\right), \quad i \in \nu, \ j \in \mathcal{N}_i \tag{12}$$

for vessel i of a multi-USV system $\mathbb{G}(\nu, \varepsilon)$ governed by (5) to achieve equally distributed surrounding motion toward a target $q_0(t) \in \mathbb{R}^2$ with a constant velocity $\dot{q}_0(t) = v_0$, subject to $\lim_{t\to\infty} e_i(t) = 0$.

If $v_0 = 0$, then Problems 1 and 2 reduce to surrounding control and equally surrounding control for a static target, respectively.

To address the high-level collective surrounding control problem, one needs to regulate each vessel to a desirable velocity $\{\psi_i^r, u_i^r, v_i^r\}$, as follows.

Problem 3 *(Individual Regulation):* Design a control protocol $\boldsymbol{\tau} = (\tau_{iu}, \tau_{ir})^\mathsf{T}$ for each vessel in a multi-USV system governed by (3) such that $\lim_{t\to\infty} \psi_i = \psi_i^r$, $\lim_{t\to\infty} u_i = u_i^r$, $\lim_{t\to\infty} v_i = v_i^r$, and $\lim_{t\to\infty} e_i = 0$.

Problem 3 could be dealt with by our previous work [30], and hence the present study will focus on the high-level collective control Problems 1 and 2 to find desirable signals $\mathbf{u}_i^r := [\psi_i^{r\mathsf{T}}, u_i^{r\mathsf{T}}, v_i^{r\mathsf{T}}]^\mathsf{T}$.

III. Surrounding Control for a Moving Target

To address Problem 1 it needs to design a distributed estimator for each vessel for estimating the states of the moving target $\dot{q}_0(t) = v_0 \in \mathbb{R}^2$ based on the intermittent neighboring information. Afterward, the estimated states $\widehat{q}_0^i, \widehat{v}_0^i$ will be used for designing the feedback control $\mathbf{u}_i^r$ of vessel i.

The distributed controller is shown in Fig. 2. In Step 1, the control law $\mathbf{u}_i^r$, or the desirable individual velocities

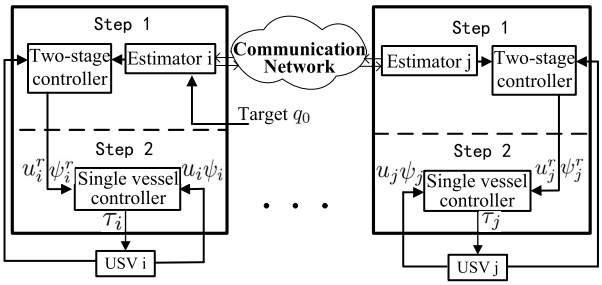

Fig. 2. Two-level surrounding controller structure of the multi-USV system, where USV i has access to the target q_0 but USV j does not.

u_i^r, v_i^r and moving direction ψ_i^r are calculated according to $f(q_i, q_j)$ and the estimate $\widehat{q}_0^i$. Then, an individual control law is designed to address Problem 3 in Step 2.

To proceed further investigation, two assumptions are in order below.

Assumption 1 Initially, the USVs with $\mathbb{G}(\nu, \varepsilon)$ are all placed within a circle with sensing radius R, that is $\|q_i(0) - q_j(0)\| \leq 2R,\ i, j \in \nu$. ■

Assumption 2 At least one vessel in the multi-USV system $\mathbb{G}(\nu, \varepsilon)$ has access to the target q_0, or $B(t)$ always has least one entry $b_i(t) \neq 0$. ■

A. Estimation of the Target State

Let $\widehat{q}_0^i(t), \widehat{v}_0^i(t)$ be the target's position $q_0(t)$ and velocity v_0 estimated by USV i, respectively, which are designed according to [31] as

$$\begin{aligned}\dot{\widehat{q}}_0^i(t) &= -k_1\left[\sum_{j\in\mathcal{N}_i}\left(\widehat{q}_0^i(t) - \widehat{q}_0^j(t)\right) + b_i(t)\left(\widehat{q}_0^i(t) - q_0(t)\right)\right] \\ &\quad + \widehat{v}_0^i(t) \\ \dot{\widehat{v}}_0^i(t) &= -\gamma k_1\left[\sum_{j\in\mathcal{N}_i}\left(\widehat{q}_0^i(t) - \widehat{q}_0^j(t)\right) + b_i(t)\left(\widehat{q}_0^i(t) - q_0(t)\right)\right].\end{aligned} \tag{13}$$

Let $\widehat{q}_0(t) := [\widehat{q}_0^1(t)^\mathsf{T}, \widehat{q}_0^2(t)^\mathsf{T}, \ldots, \widehat{q}_0^n(t)^\mathsf{T}]^\mathsf{T}, \widehat{v}_0(t) := [\widehat{v}_0^1(t)^\mathsf{T}, \widehat{v}_0^2(t)^\mathsf{T}, \ldots, \widehat{v}_0^n(t)^\mathsf{T}]^\mathsf{T} \in \mathbb{R}^{2n}$, and rewrite (13) in a compact form as

$$\begin{aligned}\dot{\widehat{q}}_0(t) &= -k_1(L_\mathbb{G}(t) + B(t)) \otimes I_2\widehat{q}_0 + (k_1 B(t) \otimes I_2) \\ &\quad \times \mathbf{1}_n \otimes q_0 + \widehat{v}_0 \\ \dot{\widehat{v}}_0(t) &= -\gamma k_1(L_\mathbb{G}(t) + B(t)) \otimes I_2\widehat{q}_0 + (\gamma k_1 B(t) \otimes I_2) \\ &\quad \times \mathbf{1}_n \otimes q_0.\end{aligned} \tag{14}$$

Lemma 1 [31]: For a first-order MAS with a moving target $q_0(t)$ and estimator governed by (14) with $0 < \gamma < 1$ and

$$k_1 \geq \frac{1}{4\gamma\left(1-\gamma^2\right)\overline{\lambda}} \tag{15}$$

where $\overline{\lambda} = \min\{\lambda(L_\mathbb{G} + B(t))$, if Assumption 2 holds and $\mathbb{G}$ is jointly dwellingly connected (see Definition 3), then the error of estimators converges to zero

$$\lim_{t\to\infty}\widetilde{q}_0^i(t) = 0, \quad \lim_{t\to\infty}\widetilde{v}_0^i(t) = 0 \tag{16}$$

with $\widetilde{q}_0^i := \widehat{q}_0^i - q_0$ and $\widetilde{v}_0^i := \widehat{v}_0^i - v_0$.

According to Lemma 1, the estimator $\widehat{q}_0^i(t), \widehat{v}_0^i(t)$ converges to the target $q_0(t)$ and v_0, respectively, with the network $\mathbb{G}$ causally disconnected. Hence, the robustness to casual communication failures has been improved when compared to the literature [30].

B. Target Surrounding Control—Stage 1

With the estimates $\widehat{q}_0^i, \widehat{v}_0^i$ in (14), the objective becomes designing a control law $\mathbf{u}_i^r = f(q_i, q_j, \widehat{q}_0^i, \widehat{v}_0^i, \mathbb{G}), i, j \in \nu$, to guide vessel i into a convex hull $\text{co}(\nu)$ around the moving target $q_0(t)$, subject to $\lim_{t\to\infty} e_i(t) = 0$. To this end, a distributed control law $\mathbf{u}_i^r$ is designed as

$$\mathbf{u}_i^r = \widehat{q}_0^i + \delta_i - q_i + \widehat{v}_0^i \tag{17}$$

with $\delta_i := \delta[\cos\ ((2\pi i)/n + \theta_0), \sin\ ((2\pi i)/n + \theta_0)]^\mathsf{T}$, $\delta = \max\|q_i(0) - q_j(0)\|, i, j \in \nu$.

Now, the main technical result concerning Problem 1 is established.

Theorem 1 For the system governed by Eqs. (5), (13), and (17) under Assumptions 1 and 2, Problem 1 with a moving target $\dot{q}_0(t) = v_0$ is solved if $\lim_{t\to\infty} e_i(t) = 0$ and the network $\mathbb{G}(t)$ is jointly dwellingly connected. ■

Proof: Let $z_i := q_i - q_0 - \delta_i$. Then, one has

$$\dot{z}_i = \dot{q}_i - v_0. \tag{18}$$

Substituting (5) into (18) yields

$$\dot{z}_i = \mathbf{u}_i^r + e_i - v_0. \tag{19}$$

Then, the closed-loop system (19) can be written as

$$\begin{aligned}\dot{z}_i &= \widehat{q}_0^i + \delta_i - q_i + \widehat{v}_0^i + e_i - v_0 \\ &= q_0 + \delta_i - q_i + \widetilde{e}_i \\ &= -z_i + \widetilde{e}_i\end{aligned} \tag{20}$$

where $\widetilde{e}_i = \widetilde{q}_0^i + \widetilde{v}_0^i + e_i$ and $\widetilde{q}_0^i := \widehat{q}_0^i - q_0$, $\widetilde{v}_0^i := \widehat{v}_0^i - v_0$ are estimated errors. It follows from Lemma 1 that $\lim_{t\to\infty}[\widetilde{q}_0^i(t)^\mathsf{T}, \widetilde{v}_0^i(t)^\mathsf{T}]^\mathsf{T} = \mathbf{0}$, which implies that $\lim_{t\to\infty}\widetilde{e}_i(t) = 0$. Rewrite (20) in a compact form as

$$\dot{z} = -z + \widetilde{e} \tag{21}$$

with $z = [z_1, z_2, \ldots, z_n]^\mathsf{T}$ and $\widetilde{e} = [\widetilde{e}_1, \widetilde{e}_2, \ldots, \widetilde{e}_n]^\mathsf{T} \in \mathbb{R}^n$. Pick a Lyapunov function $V(z) = (1/2)z^\mathsf{T}z$, satisfying

$$\begin{aligned}\dot{V}(z) &= -z^\mathsf{T}z + z^\mathsf{T}\widetilde{e} \\ &\leq -\|z\|^2 + \|z\| \cdot \|\widetilde{e}\| \\ &\leq -(1-c_1)\|z\|^2 + \|z\|(\|\widetilde{e}\| - c_1\|z\|)\end{aligned} \tag{22}$$

with $c_1 \in (0, 1)$. Then, one has $\dot{V}(z) \leq -(1-c_1)\|z\|^2, \forall\|z\| \geq (\|\widetilde{e}\|/c_1)$. If $\|z(0)\| \geq (\|\widetilde{e}\|/c_1)$, then $\dot{V}(z) \leq 0$, which implies that $\|z(t)\|$ converges into the ball of radius $(\|\widetilde{e}\|/c_1)$. If $\|z(0)\| < (\|\widetilde{e}\|/c_1)$, it is clear that $\|z(0)\|$ has already been in the ball of radius $(\|\widetilde{e}\|/c_1)$. Both cases satisfy the definition of input-to-state stability (ISS) [32], which implies that $\|z(0)\|$ could be randomly picked. Accordingly, the closed-loop system (21) is ISS with respect to $\widetilde{e}$ that satisfies

$$\|z(t)\| \leq \beta(\|z(0\|, t)) + \gamma\left(\sup_{0\leq\tau\leq t}\|\widetilde{e}(\tau)\|\right) \quad \forall t > 0 \tag{23}$$

where $\beta(\cdot)$ is a $\mathcal{KL}$ function and $\kappa_1 = (1/c_1)$ is the gain of the system (see [33]). Due to $\lim_{t\to\infty}\widetilde{e}_i(t) = 0$ and the $\mathcal{KL}$ function satisfies $\lim_{t\to\infty}\beta(\|z(0\|,t)) = 0$, it follows that $\lim_{t\to\infty} z_i(t) = 0$ in (23). Moreover, one has

$$\lim_{t\to\infty}\sum_{i=1}^{n}\frac{1}{n}q_i = \lim_{t\to\infty}\frac{1}{n}\sum_{i=1}^{n}(z_i + q_0 + \delta_i) = \lim_{t\to\infty}\sum_{i=1}^{n}\frac{1}{n}q_0 = q_0 \tag{24}$$

which implies that the target q_0 is surrounded by n USVs in a convex hull $co(v)$ and thus Problem 1 is sovled. This completes the proof. □

Remark 1 The estimator $\widehat{q}_0^i(t)$, $\widehat{v}_0^i(t)$ in (13) converges to moving target $\dot{q}_0(t) = v_0$ with the position of target $q_0(t)$ if the connection network $\mathbb{G}$ is jointly dweillingly connected, that is $T_c \geq \mu T$; otherwise, the estimator $\widehat{q}_0^i(t)$, $\widehat{v}_0^i(t)$ is unstable. It is noted that each leader USV (i.e., a USV having possible access to the target according to the communication topology) sends the estimated leader states (the information about velocity and position, but not necessarily exactly) to their neighbors, which is continuous and complete for controller design. In this way, the convergence of the target state estimator and the asymptotical stability of the closed-loop system could be guaranteed.

C. Equally Cyclically Surrounding Control—Stage 2

Problem 1 is solved in Stage 1 above for a moving target $q_0(t)$, where all the vessels surround the target $q_0(t)$ in a convex hull. Now, to solve Problem 2, a second stage control law $\mathbf{u}_i^r = f(q_i, q_j, \widehat{q}_0^i, \widehat{v}_0^i, \mathbb{G})$ is proposed as

$$\mathbf{u}_i^r = k_2(r - \widehat{\rho}_i)s_{\widehat{\theta}_i} + \widehat{\rho}_i\big(\widehat{\theta}_{i+} - \widehat{\theta}_i + \xi_i\big)t_{\widehat{\theta}_i} + \widehat{v}_0^i \tag{25}$$

where parameter $k_2 > 0$, r and ξ_i are given in Definition 2, $\widehat{\rho}_i := \|q_i - \widehat{q}_o^i\|$, and $\widehat{\theta}_i$ is the relative angle from vessel i to the estimated target $\widehat{q}_0^i$. Here, θ_{i+} is accessible as the target has been encircled by the USVs, where each vessel can detect its next-neighbor as defined in Fig. 1.

The main technical result concerning Problem 2 is established as follows.

Theorem 2 For the system governed by Eqs. (5) and (25), Problem 2 with a moving target $\dot{q}_0(t) = v_0$ is solved, that is,

1) $\lim_{t\to\infty}\rho_i = r, \quad i = 1, 2, \ldots, n;$
2) $\lim_{t\to\infty}\theta_{i+} - \theta_i + \xi_i = \lim_{t\to\infty}\theta_{j+} - \theta_j + \xi_j, \quad i, j \in v, i \neq j$

if $\lim_{t\to\infty} e_i(t) = 0$ and the network $\mathbb{G}(t)$ is jointly dwellingly connected. ■

Proof: According to the definitions of ρ_i, θ_i in Fig. 1, one has

$$q_i = \rho_i s_{\theta_i} + q_0. \tag{26}$$

Meanwhile, it follows from (18) that

$$\dot{z}_i = \dot{\rho}_i s_{\theta_i} + \rho_i t_{\theta_i}\dot{\theta}_i = J(\theta_i)\begin{bmatrix}\dot{\rho}_i \\ \rho_i\dot{\theta}_i\end{bmatrix}. \tag{27}$$

Since q_i can also be rewritten as $q_i = \widehat{\rho}_i s_{\widehat{\theta}_i} + \widehat{q}_0^i$, which implies $\lim_{t\to\infty}\widehat{\rho}_i = \rho_i$, $\lim_{t\to\infty}\widehat{\theta}_i = \theta_i$, and $\lim_{t\to\infty}\widehat{\theta}_{i+} = \theta_{i+}$, if $\lim_{t\to\infty}\widehat{q}_0^i(t) = q_0(t)$.

Substituting (25) into the closed-loop system (19) yields

$$\begin{aligned}\dot{z}_i &= \mathbf{u}_i^r + e_i \\ &= k_2(r - \rho_i + \rho_i - \widehat{\rho}_i)\big(s_{\theta_i} + s_{\widehat{\theta}_i} - s_{\theta_i}\big) \\ &\quad + (\rho_i + \widehat{\rho}_i - \rho_i)\big(\theta_{i+} - \theta_i + \xi_i + \widehat{\theta}_{i+} - \widehat{\theta}_i - \theta_{i+} + \theta_i\big) \\ &\quad \times \big(t_{\theta_i} + t_{\widehat{\theta}_i} - t_{\theta_i}\big) + \widehat{v}_0^i + e_i - v_0 \\ &= k_2(r - \rho_i)s_{\theta_i} + \rho_i(\theta_{i+} - \theta_i + \xi_i)t_{\theta_i} + \widetilde{e}_i\end{aligned} \tag{28}$$

where $\widetilde{e}_i := k_2(r - \rho_i)(s_{\widehat{\theta}_i} - s_{\theta_i}) + k_2(\rho_i - \widehat{\rho}_i)s_{\widehat{\theta}_i} + \rho_i(\widehat{\theta}_{i+} - \widehat{\theta}_i - \theta_{i+} + \theta_i)t_{\widehat{\theta}_i} + (\widehat{\rho}_i - \rho_i)(\widehat{\theta}_{i+} - \widehat{\theta}_i + \xi_i)t_{\widehat{\theta}_i} + \widehat{v}_0^i + e_i - v_0$. From Lemma 1, it follows that $\lim_{t\to\infty}\widehat{q}_0^i(t) = q_0(t), \lim_{t\to\infty}\widehat{v}_0^i(t) = v_0$, which implies that $\lim_{t\to\infty}s_{\widehat{\theta}_i}(t) - s_{\theta_i}(t) = 0, \lim_{t\to\infty}\rho_i(t) - \widehat{\rho}_i(t) = 0, \lim_{t\to\infty}\widehat{\theta}_i(t) - \theta_i(t) = 0$, and $\lim_{t\to\infty}\widehat{\theta}_{i+}(t) - \theta_{i+}(t) = 0$. Therefore, one has $\lim_{t\to\infty}\widetilde{e}_i(t) = 0$. Analogously, denoting

$$\widetilde{e}_i := J(\theta_i)\begin{bmatrix}\widehat{\eta}_i \\ \rho_i\widehat{\omega}_i\end{bmatrix} \tag{29}$$

with $\lim_{t\to\infty}\widehat{\eta}_i(t) = 0, \lim_{t\to\infty}\widehat{\omega}_i(t) = 0$ (see, [30]), it follows from (19), (25), and (29) that

$$z_i = J(\theta_i)\begin{bmatrix}k_2(r - \rho_i) + \widehat{\eta}_i \\ \rho_i(\theta_{i+} - \theta_i + \xi_i) + \rho_i\widehat{\omega}_i\end{bmatrix}. \tag{30}$$

Besides, from (27) and (28), one has

$$\begin{cases}\dot{\rho}_i = k_2(r - \rho_i) + \widehat{\eta}_i \\ \dot{\theta}_i = \theta_{i+} - \theta_i + \xi_i + \widehat{\omega}_i.\end{cases} \tag{31}$$

Define the equally cyclic surrounding errors as

$$\begin{cases}\widetilde{\rho}_i := r - \rho_i \\ \widetilde{\theta}_i := \dfrac{2\pi}{n} - (\theta_{i+} - \theta_i + \xi_i)\end{cases} \tag{32}$$

with

$$\begin{aligned}\rho &= [\rho_1, \rho_2, \ldots, \rho_n]^{\mathsf{T}}, \widetilde{\rho} = [\widetilde{\rho}_1, \widetilde{\rho}_2, \ldots, \widetilde{\rho}_n]^{\mathsf{T}} \\ \theta &= [\theta_1, \theta_2, \ldots, \theta_n]^{\mathsf{T}}, \widetilde{\theta} = \big[\widetilde{\theta}_1, \widetilde{\theta}_2, \ldots, \widetilde{\theta}_n\big]^{\mathsf{T}} \\ \xi &= [\xi_1, \xi_2, \ldots, \xi_n]^{\mathsf{T}}, \widehat{\eta} = [\widehat{\eta}_1, \widehat{\eta}_2, \ldots, \widehat{\eta}_n]^{\mathsf{T}}.\end{aligned}$$

Then, (32) can be rewritten in a compact form, as

$$\begin{cases}\widetilde{\rho} = \mathbf{1}_n \otimes r - \rho \\ \widetilde{\theta} = \mathbf{1}_n \otimes \dfrac{2\pi}{n} - (-L\theta + \xi)\end{cases} \tag{33}$$

with

$$L = \begin{bmatrix}1 & -1 & 0 & \cdots & 0 \\ 0 & 1 & -1 & 0 & \cdots \\ 0 & 0 & \cdots & \cdots & \cdots \\ -1 & 0 & \cdots & \cdots & 1\end{bmatrix}. \tag{34}$$

Its derivative is

$$\begin{cases}\dot{\widetilde{\rho}} = -k_2\widetilde{\rho} + \widetilde{\eta} \\ \dot{\widetilde{\theta}} = -L\widetilde{\theta} + \widetilde{\omega}\end{cases} \tag{35}$$

with $\widetilde{\eta} = -\widehat{\eta}, \widetilde{\omega} = -L\omega$. Condition $\lim_{t\to\infty}\widehat{\eta}_i(t) = 0$ together with $\lim_{t\to\infty}\widehat{\omega}_i(t) = 0$ implies $\lim_{t\to\infty}\widetilde{\eta}_i(t) = 0, \lim_{t\to\infty}\widetilde{\omega}_i(t) = 0$.

It follows from (10) that $\mathbf{1}_n^{\mathsf{T}}\xi = 2\pi$. Moreover, from (32), the equality holds, giving

$$\mathbf{1}_n^{\mathsf{T}}\widetilde{\theta} = \mathbf{1}_n^{\mathsf{T}}\left(\mathbf{1}_n \otimes \frac{2\pi}{n} - (-L\theta + \xi)\right) = 2\pi - 2\pi = 0. \quad (36)$$

According to [34], one has

$$\min_{\mathbf{1}_n^{\mathsf{T}}\widetilde{\theta}=0,\quad \widetilde{\theta}\neq 0} \frac{\widetilde{\theta}^{\mathsf{T}} L \widetilde{\theta}}{\|\widetilde{\theta}\|^2} = \lambda_2(L) > 0 \quad (37)$$

with $\lambda_2(L)$ being the second smallest eigenvalue of L. Let $\chi = \min\{k_2, \lambda_2(L)\} > 0$, and define

$$\varepsilon := \begin{bmatrix} \widetilde{\rho} \\ \widetilde{\theta} \end{bmatrix}, \quad \widetilde{\gamma} := \begin{bmatrix} \widetilde{\eta} \\ \widetilde{\omega} \end{bmatrix}. \quad (38)$$

Clearly, one has $\lim_{t\to\infty} \widetilde{\gamma}(t) = 0$ if $\lim_{t\to\infty} \widetilde{\eta}(t) = 0$ and $\lim_{t\to\infty} \widetilde{\omega}(t) = 0$. Pick a Lyapunov function $V(\varepsilon) = 1/2\varepsilon^{\mathsf{T}}\varepsilon$, satisfying

$$\begin{aligned} \dot{V}(\varepsilon) &= \widetilde{\rho}^{\mathsf{T}}\dot{\widetilde{\rho}} + \widetilde{\theta}^{\mathsf{T}}\dot{\widetilde{\theta}} \\ &= -k_2\widetilde{\rho}^{\mathsf{T}}\widetilde{\rho} + \widetilde{\rho}^{\mathsf{T}}\widetilde{\eta} + \widetilde{\theta}^{\mathsf{T}}\left(-L\widetilde{\theta} + \widetilde{\omega}\right) \\ &\le -k_2\|\widetilde{\rho}\|^2 - \lambda_2(L)\|\widetilde{\theta}\|^2 + \varepsilon^{\mathsf{T}}\widetilde{\gamma} \\ &\le -\chi\left(\|\widetilde{\rho}\|^2 + \|\widetilde{\theta}\|^2\right) + \|\varepsilon\| \cdot \|\widetilde{\gamma}\| \\ &\le -\chi(1-c_2)\|\varepsilon\|^2 + \|\varepsilon\|\left(\|\widetilde{\gamma}\| - \chi c_2\|\varepsilon\|\right) \end{aligned} \quad (39)$$

with $c_2 \in (0,1)$. Then, one has that $\dot{V}(\varepsilon) \le -\chi(1-c_2)\|\varepsilon\|^2$, $\forall \|\varepsilon\| \ge (\|\widetilde{\gamma}\|/\chi c_2)$. Analogously, the closed-loop system of ε is ISS with respect to $\widetilde{\gamma}$ and satisfies

$$\|\varepsilon(t)\| \le \beta(\|\varepsilon(0\|, t)) + \gamma\left(\sup_{0\le\tau\le t} \|\widetilde{\gamma}(\tau)\|\right) \quad \forall t > 0 \quad (40)$$

where $\beta(\cdot)$ is a $\mathcal{KL}$ function and $\kappa_2 = 1/(\chi c_2)$ is the gain of the system (see [33]). It follows from $\mathcal{KL}$ function $\beta(\|\varepsilon(0\|, t))$ and (38) that

$$\lim_{t\to\infty} \beta(\|\varepsilon(0\|, t)) = 0, \quad \lim_{t\to\infty} \|\widetilde{\gamma}(t)\| = 0. \quad (41)$$

Accordingly, one has $\lim_{t\to\infty} \varepsilon(t) = 0$, that is,

$$\lim_{t\to\infty} \widetilde{\rho}_i(t) = 0, \quad \lim_{t\to\infty} \widetilde{\theta}_i(t) = 0 \quad (42)$$

which implies that $\lim_{t\to\infty} \rho_i = r$ and $\lim_{t\to\infty}(\theta_{i+} - \theta_i + \xi_i) = (2\pi/n)$, that is,

$$\lim_{t\to\infty} \theta_{i+} - \theta_i + \xi_i = \lim_{t\to\infty} \theta_{j+} - \theta_j + \xi_j, \quad i, j \in \nu, i \neq j \quad (43)$$

subject to $\lim_{t\to\infty} \widehat{\eta}_i(t) = 0$ and $\lim_{t\to\infty} \widehat{\omega}_i(t) = 0$. This completes the proof. □

Remark 2 : Conditions $\lim_{t\to\infty} \widehat{\eta}_i(t) = 0$ and $\lim_{t\to\infty} \widehat{\omega}_i(t) = 0$, i.e., $\lim_{t\to\infty} \widetilde{e}_i(t) = 0$, decouples high-level collective behavior control and low-level underactuated dynamics control, which are assumed to hold for Problems 1 and 2. Problem 3 can be solved with our previous designed controller in [30]. ■

Remark 3 It follows from Theorem 1 that vessels switch to Stage 2 if Problem 1 is sovled, i.e., $\lim_{t\to\infty} z_i = 0$. To accelerate the process in real experiments, the switching condition between Stages 1 and 2 need to be satisfied if $\|z_i\| \le \sigma, i \in \nu$, with a prescribed boundary $\sigma > 0$ for the asymptotical convergence of $\|z_i\|$ in (19). ■

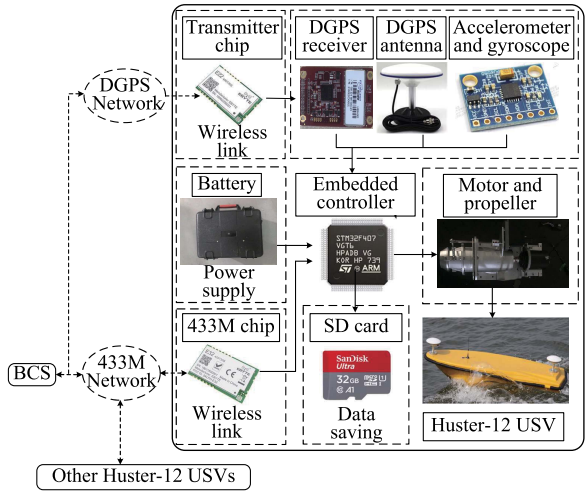

Fig. 3. Hardware structure of the multi-Huster-12s USVs.

IV. Experiments

We have applied the proposed surrounding control schemes (13), (17), and (25) to our own lake-based multi-USV platform composed of three HUSTER-12s vessels, namely a base control station (BCS), a virtual motional target vessel, and a USV dock.

As shown in Fig. 3, each HUSTER-12s USV is 1.6 meters long, with dynamic model parameters in (3) as $m_{11} = 1000.00$ kg, $m_{22} = 0.60$ kg, $m_{33} = 263.16$ kgm^2, $d_{11} = 980.40$ kgs^{-1}, $d_{22} = 0.59$ kgs^{-1}, and $d_{33} = 257.61$ kgm^{2}s^{-1}. Each vessel is equipped with an onboard differential GPS (DGPS) receivers (NovAtel-OEM615), a DGPS wireless sensor (E32-400T20S), two DGPS antennas, a 433 M wireless sensor (E32-433T30S), an accelerometer-gyroscope (AG) chip (MPU6050), an embedded controller (STM32F407VGT6), a motor driver (SEAKING-V3), a high power battery (RUIYI-48), and a waterjet propeller (HJ-064). The AG chip is embedded to navigate the vessel. Normally, with the onboard DGPS receiver and DGPS station, each USV detects its heading angle and position with accuracy ± 2 cm, which are sent to the embedded controller to yield an actuator signal. With communication of the intermittent neighboring information transferred by the 433 M wireless sensor and receiver, each USV calculates its control signal executed by a motor driver, which regulates the water-jet engine (2 kw) and the rudder with ($\pm 15°$) to fulfill the aforementioned two-stage surrounding control mission. The status trajectories of vessels and the corresponding controller parameters are all recorded by an onboard SD card (32 GB). Table I summaries the parameters of the main components and hardware of the multi-USV system.

In this experiment, three vessels are initially randomly distributed in a $[20 \times 20]$ m^2 lake area, with sensing radius R set to 18 m and encircling radius r set to 18 m. The initial states of the vessels are naturally set as $u_i = 0$ m/s, $v_i = 0$ m/s, and $r_i = 0$ rad/s. The calculated control signal is updated by the embedded controller with a sampling and updating frequency of 4 Hz. As for the moving target $q_0(t)$, the initial position is set as $q_0 = [-9510, 12010]^{\mathsf{T}}$ cm and the velocity is set as $v_0 = [-50, 50]^{\mathsf{T}}$ cm/s, both in the

TABLE I

MAIN COMPONENTS IN THE MULTI-USV SYSTEM

Component/hardware	Parameter
NovAtel-OEM615	Accuracy: $\pm 2cm$
E32-400T20S	Power: 10-20dBm, distance: 3km
E32-433T30S	Power: 21-30dBm, distance: 8km
MPU6050	Gyroscope range: $\pm 250, 500, 1000, 2000^\circ/s$, acceleration range: $\pm 2g, \pm 4g, \pm 8g, \pm 16g$
STM32F407VGT6	Flash: 1024kB, frequency: 72M, pin:100
SEAKING-V3	Voltage: 5-12s Lipo (21-50.4V), current: 130A
RUIYI-48	Capacity: 48V, 30Ah
HJ064	Power: 3.6kW, thrust: 115N

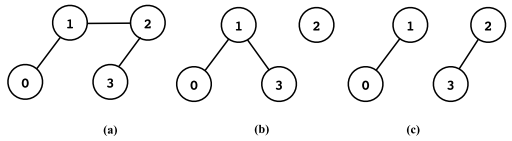

Fig. 4. Switching inter-vessel communication topologies of the multi-USV system. Nodes 1, 2, and 3 are the vessels and 0 is the virtual motional target. (a) $\mathbb{G}_a$, (b) $\mathbb{G}_b$, and (c) $\mathbb{G}_c$.

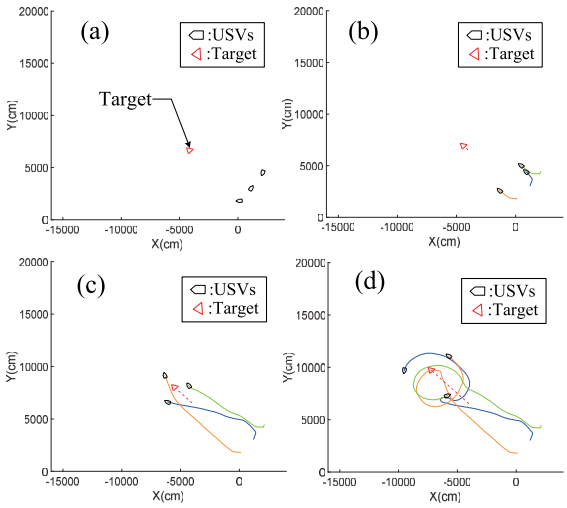

Fig. 5. Two-stage surrounding process of a virtual moving target with the multi-USV system. The colored lines are the moving trajectories of the three vessels. (a) Initial position of the USVs. (b) USVs begin to chase the virtual motional target. (c) Target has been surrounded in Stage 1. (d) USVs evenly rotate around the moving target in Stage 2.

East–North coordinate. The inter-USV intermittent communication network topology is exhibited in Fig. 4, which switches periodically following (a)–(c) with specified rate $\mu = 0.9$. If the relative distance between the visual target and the follower USVs is larger than r, the follower cannot access the virtual motional target. In such a situation, both of the two followers exchange their estimate $\widehat{q}_0^i$ with their neighbors through the onboard 433 M wireless communication network if the target is not within their sensing radius. The parameters of the controllers (13), (17), and (25) are $k_1 = 0.1$, $k_2 = 2$, $c_2 = 0.2$, $c_3 = 0.2$, $\gamma = 0.5$, which satisfy (15).

The trajectories of the two-stage surrounding control process of the vessels following the moving target $q_0(t)$ are shown in Fig. 5. As observed from Fig. 6, the distance between each vessel and the target approaches 12 m. Meanwhile, the relative angle between each pair of the neighboring vessels uniformly approaches 120° in less than 115 s, which implies

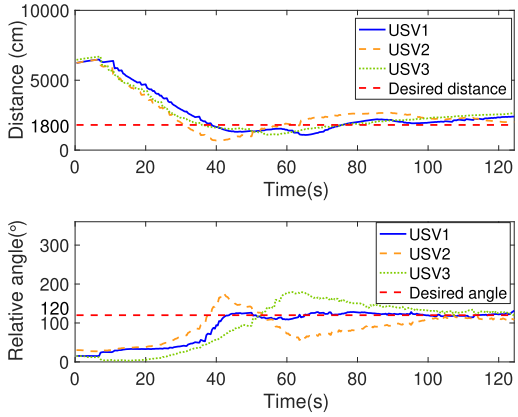

Fig. 6. Evolution of the distance and the relative angle from the vessels to the virtual moving target, respectively.

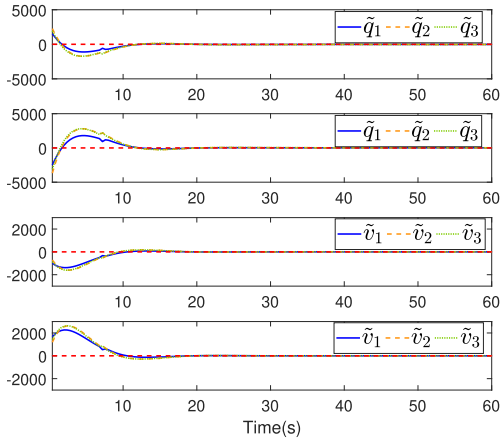

Fig. 7. Evolution of the estimated position errors $\widetilde{q}_i(t)$ and velocity errors $\widetilde{v}_i(t)$ toward the a virtual moving target, respectively.

that the three vessels capture and rotate evenly around the moving target at the center on an intermittent communication network. For the estimation errors, the evolution of the estimated state errors $\widetilde{q}_0^i, \widetilde{v}_0^i$, $i = 1, 2, 3$ [see the observer (13)] of each vessel are plotted in Fig. 7. It is observed that the estimation errors settle to zero in less than 20 seconds, which validates the feasibility of the designed observer (13). To show the surrounding control performance more vividly, a real snapshot of the equally cyclically surrounding procedure is exhibited in Fig. 8. The experiments show the effectiveness of the developed two-stage control law (17) and (25) and the feasibility of Theorems 1 and 2. Essentially, since the real experiments are conducted with intermittent communication as shown in Fig. 4, which has not been addressed by the literature [8]–[15], the superiority of the proposed control method is thus verified on the target encircling mission with evenly rotating phases, unknown target velocities, and switching communication topologies.

Note that, it generally takes a longer time for the USVs to evenly encircle a moving target, and the surrounding trajectories suffer more oscillations. This is due to the intensified external disturbances of the currents and larger communication package loss rate induced by chasing the moving target, with satisfactory performance.

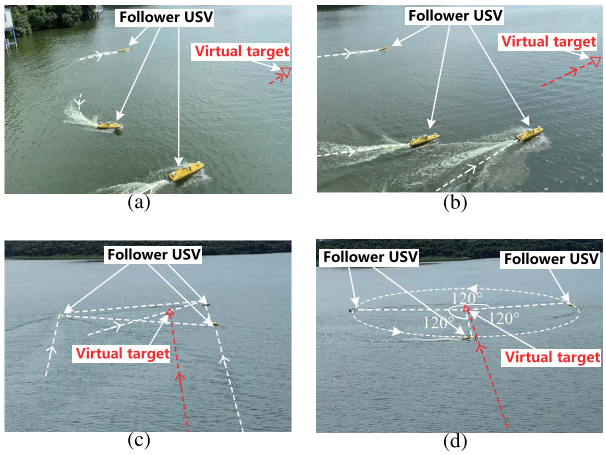

Fig. 8. Real snapshot of the two-stage equally surrounding control to follow the virtual moving target. (a) Initial position. (b) Chase the target. (c) Surround the target. (d) Rotate around the target.

V. Conclusion

In this brief, a distributed controller is proposed to address a two-stage equally surrounding problem of multi-USV systems. The virtue of the proposed controller lies in allowing for joint dwelling connectivity of the interagent communication graph, which is more realistic in practice and can effectively reduce the intervessel communication cost. Significantly, the conditions guaranteeing the asymptotical stability of the closed-loop multi-USV system are derived for the proposed surrounding controller. Finally, real lake-based experiments are conducted on three Huster-12 USVs to verify the effectiveness of the developed controller, with satisfactory performance. This brief paves the way from theoretical design to practical implementation of multi-USV systems by addressing a set of issues encountered in real applications. Future work will investigate multi-USV surrounding control for multiple moving targets with large velocity variations.

References

[1] M. Bibuli, G. Bruzzone, M. Caccia, and L. Lapierre, "Path-following algorithms and experiments for an unmanned surface vehicle," *J. Field Robot.*, vol. 26, no. 8, pp. 669–688, Aug. 2009.

[2] M. Caccia, G. Bruzzone, and R. Bono, "A practical approach to modeling and identification of small autonomous surface craft," *IEEE J. Ocean. Eng.*, vol. 33, no. 2, pp. 133–145, Apr. 2008.

[3] W. B. Klinger, I. R. Bertaska, K. D. von Ellenrieder, and M. R. Dhanak, "Control of an unmanned surface vehicle with uncertain displacement and drag," *IEEE J. Ocean. Eng.*, vol. 42, no. 2, pp. 458–476, Apr. 2017.

[4] E. Lefeber, K. Y. Pettersen, and H. Nijmeijer, "Tracking control of an underactuated ship," *IEEE Trans. Control Syst. Technol.*, vol. 11, no. 1, pp. 52–61, Jan. 2003.

[5] H. Ashrafiuon, K. R. Muske, L. C. McNinch, and R. A. Soltan, "Sliding-mode tracking control of surface vessels," *IEEE Trans. Ind. Electron.*, vol. 55, no. 11, pp. 4004–4012, Nov. 2008.

[6] W. He, Z. Yin, and C. Sun, "Adaptive neural network control of a marine vessel with constraints using the asymmetric barrier Lyapunov function," *IEEE Trans. Cybern.*, vol. 47, no. 7, pp. 1641–1651, Jul. 2017.

[7] Y.-L. Wang and Q.-L. Han, "Network-based fault detection filter and controller coordinated design for unmanned surface vehicles in network environments," *IEEE Trans. Ind. Informat.*, vol. 12, no. 5, pp. 1753–1765, Oct. 2016.

[8] Z. Peng, D. Wang, Z. Chen, X. Hu, and W. Lan, "Adaptive dynamic surface control for formations of autonomous surface vehicles with uncertain dynamics," *IEEE Trans. Control Syst. Technol.*, vol. 21, no. 2, pp. 513–520, Mar. 2013.

[9] B. Xiao, X. Yang, and X. Huo, "A novel disturbance estimation scheme for formation control of ocean surface vessels," *IEEE Trans. Ind. Electron.*, vol. 64, no. 6, pp. 4994–5003, Jun. 2017.

[10] Z. Peng, D. Wang, T. Li, and M. Han, "Output-feedback cooperative formation maneuvering of autonomous surface vehicles with connectivity preservation and collision avoidance," *IEEE Trans. Cybern.*, vol. 50, no. 6, pp. 2527–2535, Jun. 2020, doi: 10.1109/TCYB.2019.2914717.

[11] J. Ghommam and F. Mnif, "Coordinated path-following control for a group of underactuated surface vessels," *IEEE Trans. Ind. Electron.*, vol. 56, no. 10, pp. 3951–3963, Oct. 2009.

[12] K. D. Do, "Synchronization motion tracking control of multiple underactuated ships with collision avoidance," *IEEE Trans. Ind. Electron.*, vol. 63, no. 5, pp. 2976–2989, May 2016.

[13] T. Li, R. Zhao, C. L. P. Chen, L. Fang, and C. Liu, "Finite-time formation control of under-actuated ships using nonlinear sliding mode control," *IEEE Trans. Cybern.*, vol. 48, no. 11, pp. 3243–3253, Nov. 2018.

[14] Z. Peng, J. Wang, and D. Wang, "Distributed containment maneuvering of multiple marine vessels via neurodynamics-based output feedback," *IEEE Trans. Ind. Electron.*, vol. 64, no. 5, pp. 3831–3839, May 2017.

[15] Z. Peng, J. Wang, and D. Wang, "Containment maneuvering of marine surface vehicles with multiple parameterized paths via spatial-temporal decoupling," *IEEE/ASME Trans. Mechatronics*, vol. 22, no. 2, pp. 1026–1036, Apr. 2017.

[16] H. Yamaguchi, "A cooperative hunting behavior by mobile-robot troops," *Int. J. Robot. Res.*, vol. 18, no. 9, pp. 931–940, Sep. 1999.

[17] J. Ni and S. X. Yang, "Bioinspired neural network for real-time cooperative hunting by multirobots in unknown environments," *IEEE Trans. Neural Netw.*, vol. 22, no. 12, pp. 2062–2077, Dec. 2011.

[18] R. Sepulchre, D. A. Paley, and N. E. Leonard, "Stabilization of planar collective motion: All-to-all communication," *IEEE Trans. Autom. Control*, vol. 52, no. 5, pp. 811–824, May 2007.

[19] J. A. Marshall, M. E. Broucke, and B. A. Francis, "Formations of vehicles in cyclic pursuit," *IEEE Trans. Autom. Control*, vol. 49, no. 11, pp. 1963–1974, Nov. 2004.

[20] A. Sinha and D. Ghose, "Generalization of nonlinear cyclic pursuit," *Automatica*, vol. 43, no. 11, pp. 1954–1960, Nov. 2007.

[21] T.-H. Kim and T. Sugie, "Cooperative control for target-capturing task based on a cyclic pursuit strategy," *Automatica*, vol. 43, no. 8, pp. 1426–1431, Aug. 2007.

[22] N. Ceccarelli, M. Di Marco, A. Garulli, and A. Giannitrapani, "Collective circular motion of multi-vehicle systems," *Automatica*, vol. 44, no. 12, pp. 3025–3035, Dec. 2008.

[23] D. Li, G. Ma, W. He, S. S. Ge, and T. H. Lee, "Cooperative circumnavigation control of networked microsatellites," *IEEE Trans. Cybern.*, vol. 50, no. 10, pp. 4550–4555, Oct. 2020, doi: 10.1109/TCYB.2019.2923119.

[24] Y. Lan, G. Yan, and Z. Lin, "Distributed control of cooperative target enclosing based on reachability and invariance analysis," *Syst. Control Lett.*, vol. 59, no. 7, pp. 381–389, Jul. 2010.

[25] X. Yu and L. Liu, "Distributed circular formation control of ring-networked nonholonomic vehicles," *Automatica*, vol. 68, pp. 92–99, Jun. 2016.

[26] R. Zheng, Y. Liu, and D. Sun, "Enclosing a target by nonholonomic mobile robots with bearing-only measurements," *Automatica*, vol. 53, pp. 400–407, Mar. 2015.

[27] R. Li, Y. Shi, and Y. Song, "Localization and circumnavigation of multiple agents along an unknown target based on bearing-only measurement: A three dimensional solution," *Automatica*, vol. 94, pp. 18–25, Aug. 2018.

[28] X. Yu and L. Liu, "Cooperative control for moving-target circular formation of nonholonomic vehicles," *IEEE Trans. Autom. Control*, vol. 62, no. 7, pp. 3448–3454, Jul. 2017.

[29] X. Yu, X. Xu, L. Liu, and G. Feng, "Circular formation of networked dynamic unicycles by a distributed dynamic control law," *Automatica*, vol. 89, pp. 1–7, Mar. 2018.

[30] B. Liu *et al.*, "Collective dynamics and control for multiple unmanned surface vessels," *IEEE Trans. Control Syst. Technol.*, vol. 28, no. 6, pp. 2540–2547, Nov. 2020, doi: 10.1109/TCST.2019.2931524.

[31] Y. Hong, J. Hu, and L. Gao, "Tracking control for multi-agent consensus with an active leader and variable topology," *Automatica*, vol. 42, no. 7, pp. 1177–1182, Jul. 2006.

[32] H. K. Khalil, *Nonlinear Systems*. Upper Saddle River, NJ, USA: Prentice-Hall, 2002.

[33] A. Isidori, *Nonlinear Control Systems II*. Berlin, Germany: Springer, 2012.

[34] R. Olfati-Saber and R. M. Murray, "Consensus problems in networks of agents with switching topology and time-delays," *IEEE Trans. Autom. Control*, vol. 49, no. 9, pp. 1520–1533, Sep. 2004.